Chapter 5

Single-Molecule Imaging of Recycling Synaptic Vesicles in Live Neurons

Merja Joensuu, Ramon Martínez-Mármol, Mahdie Mollazade, Pranesh Padmanabhan, and Frédéric A. Meunier

Abstract

The capacity of neurons to communicate and store information in the brain critically depends on neurotransmission, a process which relies on the release of chemicals called neurotransmitters stored in synaptic vesicles at the presynaptic nerve terminals. Following their fusion with the presynaptic plasma membrane, synaptic vesicles are rapidly reformed via compensatory endocytosis. The investigation of the endocytic pathway dynamics is severely restricted by the diffraction limit of light and, therefore, the recycling of synaptic vesicles, which are roughly 45 nm in diameter, has been primarily studied with electrophysiology, low-resolution fluorescence-based techniques, and electron microscopy. Here, we describe a recently developed technique we named subdiffractional tracking of internalized molecules (sdTIM) that can be used to track and study the mobility of recycling synaptic vesicles in live hippocampal presynapses. The chapter provides detailed guidelines on the application of the sdTIM protocol and highlights controls, adaptations, and limitations of the technique.

Key words Endocytosis, Hippocampal neurons, Synaptic vesicles, Super-resolution microscopy, Single-particle tracking, Vesicle-associated membrane protein 2 (VAMP2-pHluorin), Nanobodies

1 Introduction: Activity-Dependent Internalization of Nanobodies

The recycling of synaptic vesicles is fundamental to maintain synaptic activity [1], and to promote neuronal survival [2] and presynaptic homeostasis [3]. Synaptic vesicles are highly enriched in presynaptic nerve terminals. Following Ca^{2+} influx, these vesicles fuse with the presynaptic plasma membrane releasing neurotransmitters into the synaptic cleft, thereby transmitting the information to the postsynaptic neuron. Following fusion, the vesicle membrane is retrieved from the plasma membrane by compensatory endocytosis to replenish the recycling synaptic vesicle pool. Despite appearing morphologically similar in electron micrographs, synaptic vesicles are not functionally identical, and vesicles that share similar properties (such as release probabilities) can be categorized

Nobuhiko Yamamoto and Yasushi Okada (eds.), *Single Molecule Microscopy in Neurobiology*, Neuromethods, vol. 154, https://doi.org/10.1007/978-1-0716-0532-5_5,

into distinct vesicle pools. While varied descriptions of the pools and accompanying nomenclature exist [4, 5], three major functional synaptic vesicle pools are commonly described based on their ability to undergo regulated fusion: the readily releasable pool, the recycling pool, and the reserve pool [4–9]. Synaptic vesicles can be further subcategorized into populations such as the superpool that transits rapidly between neighboring synaptic boutons and the surface pool of vesicular proteins that resides on the plasma membrane following synaptic vesicle fusion and neurosecretion [5, 10–13].

Owing to their small size [14], the details of the heterogeneous mobility patterns of individual synaptic vesicles can only be resolved by super-resolution imaging techniques [10–13, 15–20]. A detailed investigation into the cellular processes associated with these heterogeneous populations requires direct and continual tracking of multiple synaptic vesicles simultaneously, in order to collect sufficient data to robustly infer the various mobility states and parameters characterizing vesicle recycling [21]. We recently developed a novel pulse-chase-based method called *s*ub*d*iffractional *t*racking of *i*nternalized *m*olecules (sdTIM) [21, 22] that allows investigators to acquire thousands of relatively long-lasting single-molecule trajectories from recycling synaptic vesicles in the crowded live hippocampal nerve endings and adjacent axons.

sdTIM relies on the activity-dependent internalization of fluorescent ligands into endocytic compartments, such as synaptic vesicles [3, 21, 22] and endosomes [2, 22], and can also be used to track retrogradely transported autophagosomes [3]. This book chapter describes one of the applications of the sdTIM protocol to study the mobility of individual recycling synaptic vesicles in nerve terminals of live hippocampal neurons by overexpressing pHluorin-tagged vesicle-associated membrane protein 2 (VAMP2-pHluorin [23]). The activity-dependent internalization of externally applied anti-green fluorescent protein (GFP) Atto647N-labeled nanobodies (Atto647N-NBs), which bind specifically to pHluorin, is achieved by inducing depolarization with high-potassium (K^+) buffer (referred to as the "pulse"). pHluorin moiety is a pH-sensitive GFP variant [23–25] that, when fused to the C-termini of VAMP2, is quenched in the acidic intravesicular environment (pH 5.5). Following the exocytic fusion of the synaptic vesicle with the plasma membrane, the intravesicular pHluorin of VAMP2-pHluorin is exposed to the neutral (pH 7.0) extracellular space and unquenched, thereby emitting fluorescence. VAMP2-pHluorin can, therefore, be used as an optical indicator to monitor secretion and synaptic transmission and to discriminate active nerve terminals from the adjacent axonal segments. Following stimulation, neurons are then washed with low-K^+ buffer to remove any free Atto647N-NBs and incubated in low-K^+ buffer for 10 min (referred to as the "chase"). VAMP2-pHluorin-bound Atto647N-

NBs internalize into recycling synaptic vesicles, and the pHluorin is re-quenched following the subsequent reacidification of the synaptic vesicles [23–25]. Neurons are then imaged under oblique illumination to detect and track single molecules of internalized VAMP2-pHluorin-bound Atto647N-NBs. In oblique illumination, the laser beam passes through the sample at an angle slightly smaller than the critical angle which is used in total internal reflection fluorescence (TIRF) microscopy. Thus, unlike TIRF illumination which only excites a thin optical section close to the coverslip, oblique illumination allows image acquisition from a thicker optical section that extends beyond the basal surface of the neuron while not illuminating the molecules outside the evanescent wave [26, 27]. Individual synaptic vesicles containing Atto647N-NBs can then be tracked using single-particle tracking algorithms until the Atto647N-NBs either bleach or exit the field of view.

The sdTIM protocol involves the following main steps: (1) neuronal dissection and culturing from embryonic rats (or mice) (Fig. 1), (2) induction of activity-dependent internalization of Atto647N-NBs in recycling synaptic vesicles (Figs. 2 and 3),

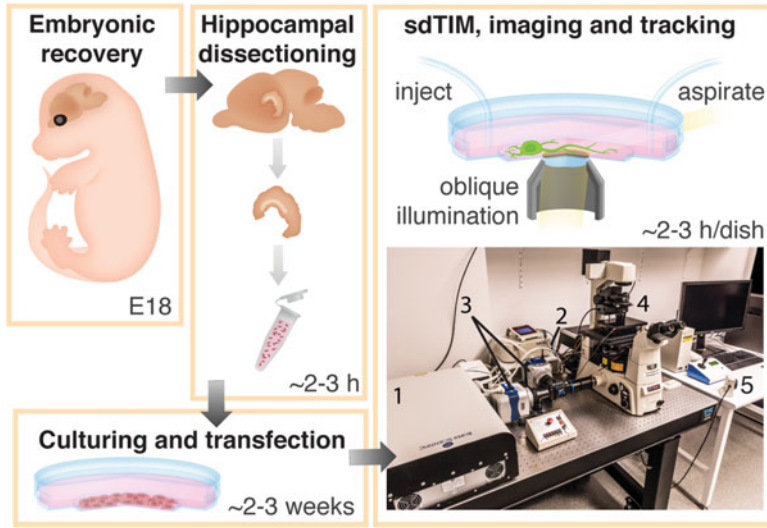

Fig. 1 The main steps of sdTIM protocol and expected duration. The protocol starts with embryonic (E18) recovery from rats, followed by dissection of the hippocampi. Hippocampal neurons are plated and cultured on super-resolution-compatible glass-bottom dishes and transfected with VAMP2-pHluorin. Induction of activity-dependent internalization of Atto647N-NBs is then performed under oblique illumination, using custom-made experimental perfusion and aspiration system [22], to image single molecules of VAMP2-pHluorin-bound Atto647N-NBs internalized in recycling synaptic vesicles. Single molecules are then tracked with single-molecule tracking software PALM Tracer in the MetaMorph software. *Bottom right*, our Roper iLas2 microscope single-particle imaging setup: lasers (1), iLas^2 (2), EMCCD cameras (3), microscope (4), and computer for image acquisition software (5) are indicated

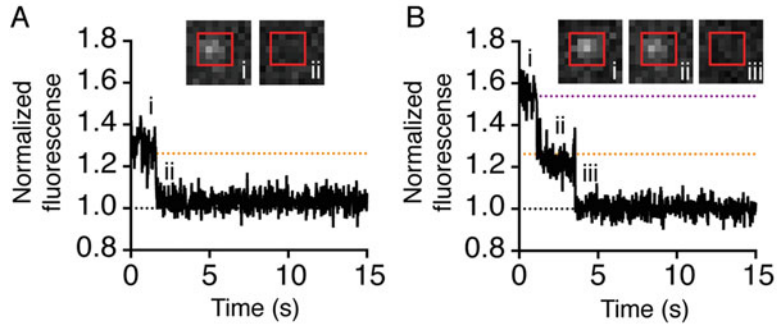

Fig. 2 Obtaining Atto647N emission curves of the anti-GFP nanobodies. (**a**) A representative intensity-time (s) trace of the time recording of Atto647N-NB deposited on a glass surface at pH 7.4. The graph shows a representative fluorescence trace from 5 × 5 pixels (red square) around the center of the Atto647N-NB during excitation (i) and after bleaching (ii), indicating a single-emission step. (**b**) The graph shows a trace of Atto647N-NB during excitation (i) and after first bleaching step (ii) and second bleaching step (iii), indicating two emission steps. The intensity-time traces are normalized to background. Dotted orange and purple lines indicate the detected emission steps. The number of internalized Atto647N-NBs inside synaptic vesicles in fixed (Subheading 3.8) and live (Subheading 3.9) neurons can be assessed similarly

(3) live-cell imaging (Fig. 3), and (4) tracking and analysis of single-particle mobility patterns (Figs. 4–7). We begin by describing the quantification of Atto647N-fluorophore labeling density of nanobodies in a cell-free system (Subheading 3.1, Fig. 2). The sdTIM protocol starts with coating of the super-resolution-compatible cell culture dishes (Subheading 3.2) and dissection of hippocampal neurons (Subheading 3.3), followed by neuronal plating (Subheading 3.4), culturing, and transfection of differentiated neurons (Subheading 3.5). Following imaging (Subheading 3.6) and single-molecule tracking (Subheading 3.7), the assessment of the number of internalized Atto647N-NBs inside synaptic vesicles in fixed (Subheading 3.8) and live (Subheading 3.9) neurons can be performed. For the validation of the sdTIM experimental setup, we also describe how to evaluate the correct targeting of internalized nanobodies using sdTIM in correlation with electron microscopy and how to assess neuronal maturity (Subheading 3.10, Fig. 8). Finally, we discuss potential sdTIM adaptations (Subheading 3.11) to study endocytosis of various biological processes using different fluorescent labels and ligands, and in combination with other super-resolution imaging techniques (e.g., single-particle tracking photoactivated localization microscopy, sptPALM).

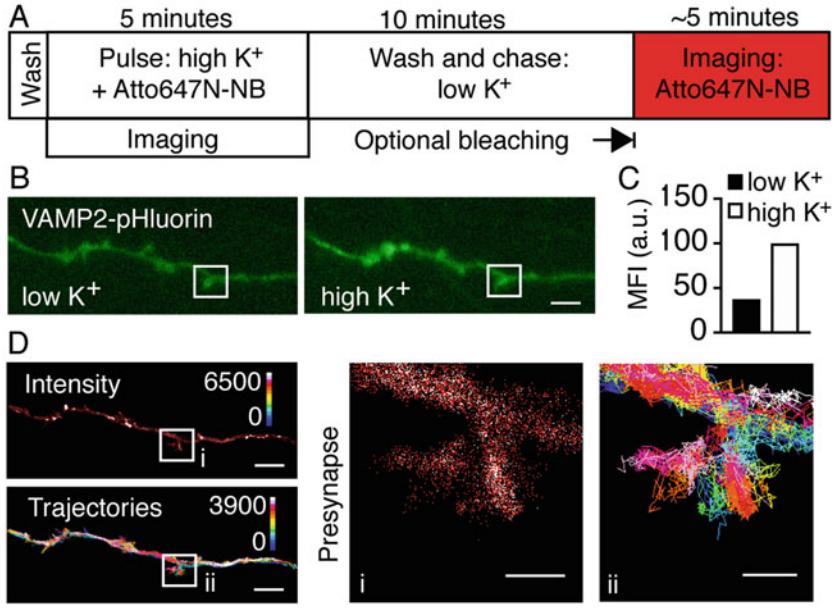

Fig. 3 Induction of activity-dependent internalization of Atto647N-NBs in recycling synaptic vesicles. (**a**) sdTIM experimental timeline. Hippocampal neurons expressing VAMP2-pHluorin are washed with low-K^+ buffer, stimulated in anti-GFP Atto647N-NB (3.2 pg/μl) containing high-K^+ buffer for 5 min (pulse), during which the unquenching of the VAMP2-pHluorin is monitored (imaging). Neurons are then washed and chased for 10 min in low-K^+ buffer. Prior to imaging, the internalized Atto647N-NBs can be partially bleached with short laser illumination (optional) to help discriminate single recycling synaptic vesicles in the highly crowded presynaptic environment. After the chase, single-molecule imaging of internalized Atto647N-NB in recycling SVs is performed under oblique illumination microscopy. (**b**) Wide-field image of hippocampal neuron expressing VAMP2-pHluorin subjected to sdTIM showing fluorescence unquenching at hippocampal presynapse (boxed ROI) following high-K^+ stimulation. (**c**) A representative measurement of the VAMP2-pHluorin fluorescence intensity (*MFI* mean fluorescence intensity, *a.u.* arbitrary unit) before stimulation (low-K^+ buffer) and following high-K^+ stimulation from the indicated presynapse in (**b**). (**d**) Corresponding super-resolved average intensity image shows the density map of internalized VAMP2-pHluorin-bound Atto647N-NB localizations. The colored bar represents localization densities, and the colder colors indicate higher density. Trajectory color coding refers to acquisition frame number. Bars, 3 μm for (**b**) and (**d**), and 750 nm for the magnified presynaptic ROIs (i, ii) on bottom right

2 Materials and Equipment

2.1 Neuronal Dissection, Culturing, and Transfection

- *Coating of the glass-bottom cell culture dishes*:

  Use poly-L-lysine hydrobromide (PLL) and boric acid (both from Sigma-Aldrich) to prepare filter-sterilized 1 mg/ml PLL in 0.1 M borate buffer pH 8.5. The 1 mg/ml PLL solution can be stored at −20 °C for up to 2 months. Use UltraPure DNase/RNase-free dH2O (Invitrogen-Thermo Fisher Scientific) for washes and storage of coated dishes.

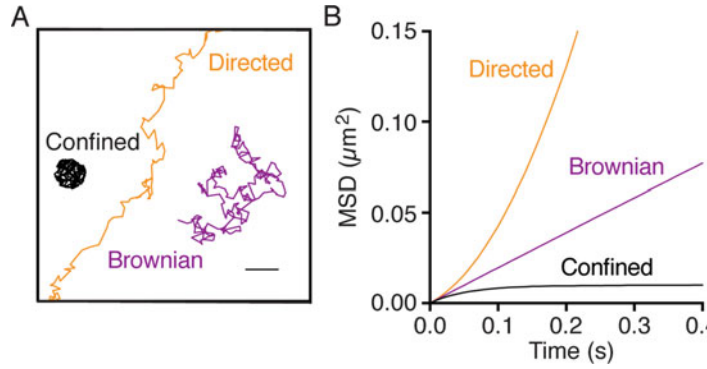

Fig. 4 In silico simulations of anticipated synaptic vesicle motion patterns. (**a**) Examples of simulation of two-dimensional particle trajectories undergoing confined (black), brownian (purple), and directed (orange) motion. Bar 200 nm. (**b**) Average MSDs of simulated particle trajectories undergoing different motion patterns. Each MSD curve is obtained from 100 simulated trajectories with 200 time steps sampled at 10-ms interval

- *Dissection medium*:
  1× Hanks' buffered salt solution without calcium, magnesium, and phenol red (HBSS) and 10 mM HEPES pH 7.3 (both from Gibco-Thermo Fisher Scientific) and 100 U/ml penicillin-100 μg/ml streptomycin (Invitrogen-Thermo Fisher Scientific). Filter-sterilize the buffer with a sterile disposable filter unit and store the buffer at 4 °C for up to 1 month.
- *Neuronal plating medium*:
  Neurobasal medium, 100 U/ml penicillin-100 μg/ml streptomycin, 1× GlutaMAX supplement, and 5% fetal bovine serum (FBS) all from Gibco-Thermo Fisher Scientific. Mix the solution well, filter-sterilize if necessary, and store at 4 °C up to the manufacturer's expiration date.
- *Neuronal culture medium*:
  Neurobasal medium, 100 U/ml penicillin-100 μg/ml streptomycin, 1× GlutaMAX supplement, and 1× B27 (Gibco-Thermo Fisher Scientific). Mix the solution well, filter-sterilize if necessary, and store at 4 °C up to the expiration date recommended by the manufacturer. Optional: The medium can be supplemented with 20% neuroglial conditioned medium (for details, *see* Joensuu et al. [22]). Furthermore, 5 μM cytosine β-D-arabinofuranoside (Ara-C; Sigma-Aldrich) can be added to the culture dish on day 3 in vitro (DIV3) to decrease the proportion of glial cells in the culture.
- *Neuronal maintenance medium*:
  Neurobasal medium, 100 U/ml penicillin-100 μg/ml streptomycin, 1× GlutaMAX supplement, and 1× B27. Mix

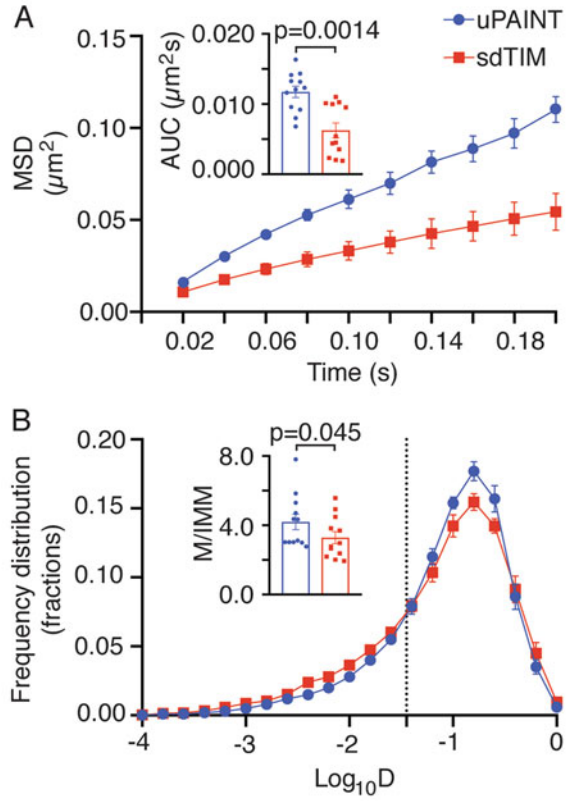

Fig. 5 Comparison of single-molecule mobility of VAMP2-pHluorin-bound Atto647N-NBs on the plasma membrane and following internalization. The comparison of VAMP2-pHluorin-bound Atto647N-NB mobility following uPAINT (i.e., on the plasma membrane; blue) and sdTIM (i.e., internalized into recycling synaptic vesicles; red) is shown as (**a**) MSD (μm^2) over time (s) and AUC (μm^2 s; inset), as well as (**b**) frequency distribution of the mean $Log_{10}D$ and mobile-to-immobile (M/IMM) ratio. The threshold for the immobile ($Log_{10}D \leq -1.45$) and mobile ($Log_{10}D > -1.45$) fraction is indicated with a dotted line in (**b**). $n = 12$ hippocampal neurons in individual cultures following sdTIM (97,400 trajectories) and uPAINT (52,800 trajectories). Statistical analyses of independent experiments were performed using Mann-Whitney *U* test (inset in **a**) and the Student's *t* test (inset in **b**). Single-molecule tracking was performed with PALM-Tracer software operating in the MetaMorph. The graphs are modified from Joensuu et al., Journal of Cell Biology 2016 with a permission from Rockefeller University Press

the solution well, filter-sterilize if necessary, and store at 4 °C up to the recommended expiry date.

- *Neuronal transfection*:

  Transfection of VAMP2-pHluorin (kindly provided by J. Rothman, Yale University [23]) is performed according to

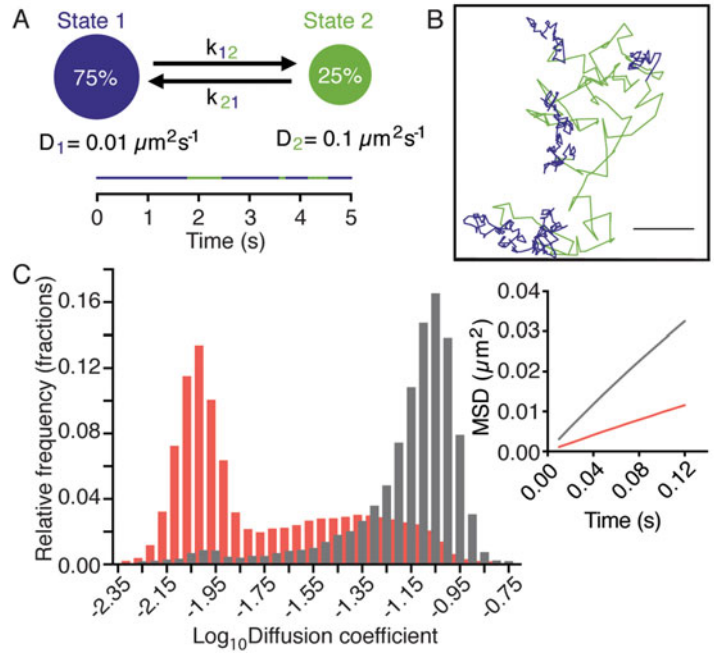

Fig. 6 Predictions of a model with two diffusive states. (**a**) A schematic of a two-state model where particle trajectories switch between two distinct diffusive states in a circular region with 500 nm radius. D_1 and D_2 are the diffusion coefficients of state 1 (blue) and state 2 (green), respectively; k_{12} is the rate of transition from state 1 to state 2; and k_{21} is the rate of transition from state 2 to state 1. Circles represent different states, and their area is proportional to the indicated percentage state occupancy over 5-s-long simulation shown in (**a**). *Bottom*, timeline showing the temporal sequence of in silico simulated particle switching between the two states shown in (**a**). (**b**) An example of a simulation of one particle switching between two diffusive states (blue and green). Bar, 200 nm. (**c**) *Left*, distribution of diffusion coefficients and, *right*, average MSDs of particles switching between the two states with $D_1 = 0.01\ \mu m^2\ s^{-1}$, $D_2 = 0.1\ \mu m^2\ s^{-1}$, $k_{12} = 1\ s^{-1}$, and $k_{12} = 4\ s^{-1}$ (red), and $D_1 = 0.01\ \mu m^2\ s^{-1}$, $D_2 = 0.1\ \mu m^2\ s^{-1}$, $k_{12} = 4\ s^{-1}$, and $k_{12} = 1\ s^{-1}$ (gray). In (**c**), each MSD curve and distribution of diffusion coefficients were obtained from 20,000 simulated trajectories with 50 time steps sampled at 10-ms intervals

the manufacturer's instructions (Lipofectamine 2000 Transfection Reagent, Invitrogen) on DIV13–16.

2.2 Atto467N Nanobodies, Beads, and Buffers for sdTIM

- *Low-K^+ buffer*:

  Prepare 0.5 mM $MgCl_2$, 2.2 mM $CaCl_2$, 5.6 mM KCl, 145 mM NaCl, 5.6 mM D-glucose, 0.5 mM ascorbic acid, 0.1% (wt/vol) bovine serum albumin (BSA), and 15 mM HEPES, pH 7.4. Measure the osmolarity using an osmometer (the osmolarity should be 290–310 mOsm). Filter-sterilize and store at 4 °C for up to 2 weeks.

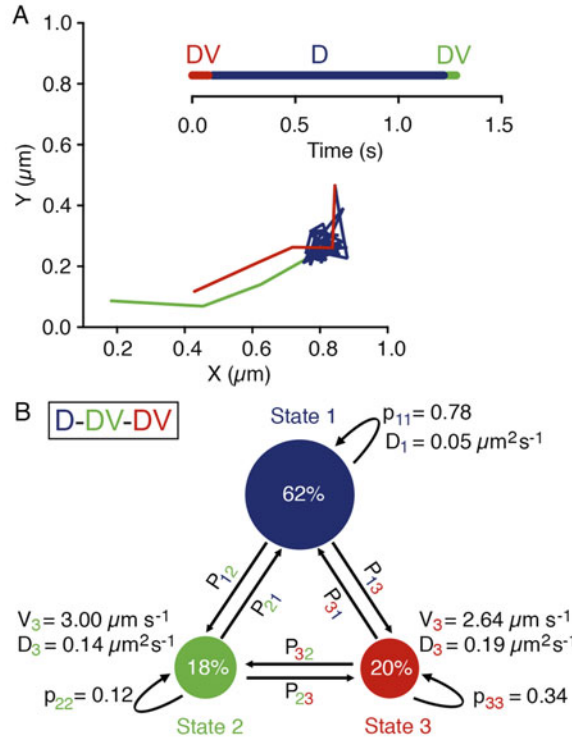

Fig. 7 HMM-Bayes analysis of the internalized VAMP2 in presynapses and axonal segments. (**a**) An example of recycling synaptic vesicle trajectory displaying D–DV–DV (D, diffusive state; DV, transport state) motion inferred by HMM-Bayes analysis. Timeline shows the order and duration (s) of the motion states in the trajectory. (**b**) Example of a three-state D–DV–DV model in a presynapse, inferred from a set of internalized VAMP2-pHluorin-bound Atto647N nanobody trajectories. Circles represent the different states, and their area is proportional to the percentage occupation of VAMP2-pHluorin-bound Atto647N nanobodies in the respective state. P_{ij}, where $i = 1$, 2, or 3 and $j = 1$, 2, or 3, are the transition probabilities, with $i = j$ indicating the probability of staying in the same state and $i \neq j$ indicating the probability of switching to another state. Apparent diffusion coefficients (D) and velocity magnitudes (V) for the states 2 and 3 are indicated. $P_{12} = 0.22$, $P_{21} = 0.30$, $P_{13} = <0.001$, $P_{31} = 0.16$, $P_{23} = 0.58$, and $P_{32} = 0.50$. Images are modified from Joensuu et al., Journal of Cell Biology 2016 with a permission from Rockefeller University Press

- *High-K^+ buffer*:

  Prepare 0.5 mM $MgCl_2$, 2.2 mM $CaCl_2$, 56 mM KCl, 95 mM NaCl, 5.6 mM D-glucose, 0.5 mM ascorbic acid, 0.1% (wt/vol) BSA, and 15 mM HEPES, pH 7.4. Measure the osmolarity using an osmometer (the osmolarity should be 290–310 mOsm). Filter-sterilize and store at 4 °C for up to 2 weeks.

- *Fluorescent beads for drift correction*:

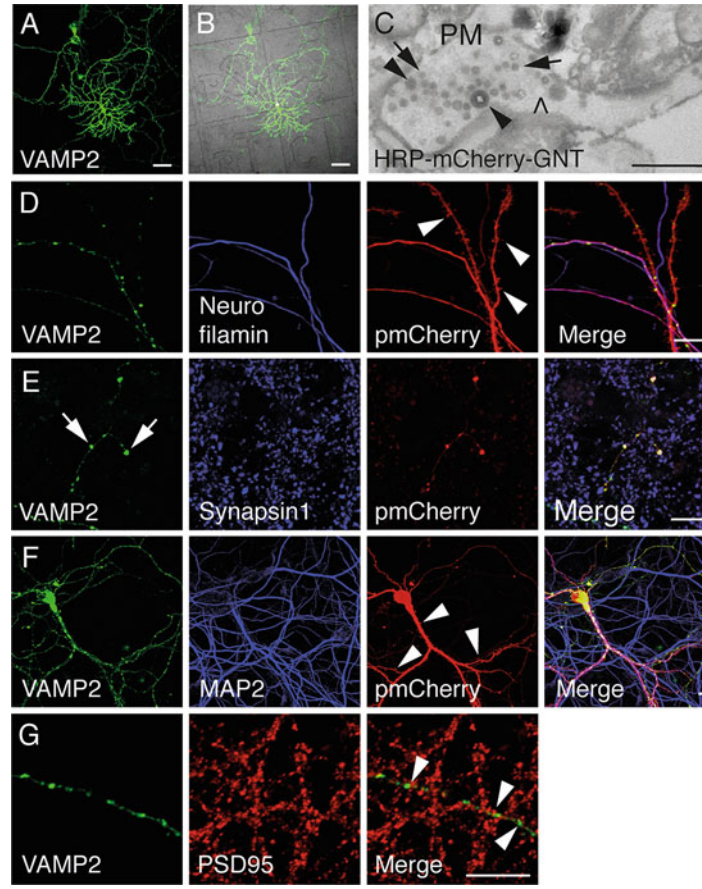

Fig. 8 Evaluation of the correct targeting of anti-GFP nanobodies with CLEM and the assessment of neuronal maturity. (**a**) Alpha numeric localization of live hippocampal neuron expressing VAMP2-pHluorin on glass-bottom grids is recorded (**b**) and neurons are then subjected to sdTIM using HRP-mCherry-GNT. (**c**) After fixation and cytochemical staining, neurons are processed for EM. The same neuron in (**a**) is correlated to the electron micrograph by following the recorded location of the neuron on the grid. HRP precipitate in recycling synaptic vesicles (arrows) and in endosomes (arrowheads) is indicated along with unstained synaptic vesicles (open arrowhead). Residual staining can be observed on the plasma membrane (PM). Bars 10 μm in (**a**, **b**, **d**–**g**) and 500 μm in (**c**). Hippocampal neurons transfected with VAMP2-pHluorin (**d**–**g**) and mCherry-C1 (**d**–**f**) and immunostained against endogenous (**d**) neurofilamin, (**e**) synapsin1, (**f**) MAP2, or (**g**) PSD95

Prepare a dilution of TetraSpeck™ Microspheres (Thermo Fisher Scientific) in low-K^+ buffer.

- *Atto647N-labeled anti-GFP nanobodies*:

  Heavy-chain antibodies from *Camelidae* sp. recognize antigens via their variable domain (referred to as V_HH or nanobody) and lack the antibody light chains [28].

A variety of labeled (e.g., Atto647N and Atto565) camelid single-domain nanobodies (also known as sdABs) with different target specificity are commercially available from Synaptic Systems. Alternatively, unlabeled anti-GFP V_HH-purified nanobodies can be purchased, for example from Chromotek, which can then be labeled with Atto647N (ATTO-TEC Gmbh) or other fluorophores as we have described previously [21, 29]. These nanobodies can recognize and bind to any protein of interest with an extracellular GFP. It will also recognize GFP-related fluorescent protein tags such as mCerulean, pHluorin, and YFP but not mCherry or red fluorescent protein (RFP). Fluorescently labeled nanobodies are light sensitive and should therefore be protected by wrapping the nanobody-containing solution tubes in aluminum foil. We recommend avoiding repetitive cycles of freezing and thawing by storing the nanobodies in small aliquots at −80 °C for up to 12 months. For best results, always prepare fresh nanobody dilution for each experiment and protect it from light.

- *Quantifying Atto647N labeling of the nanobodies*:

  Reagents required to prepare the flow chamber: 1 M potassium hydroxide, Milli-Q water, PBS, and hydrochloric acid for titration. The required volume of nanobody dilution for a flow chamber is 200 µl. Prepare 3.20 pg/µl anti-GFP Atto647N-NB dilution in phosphate-buffered saline (PBS) at pH 7.4 (or 7.0). For acidic environment tests, titrate PBS with HCl to pH 5.0 (or 5.5) and use immediately. Prepare the dilution fresh, protect it from light, and keep the dilution on ice until proceeding with the cell-free flow-chamber imaging and analysis of the Atto647N labeling density of the nanobodies (Subheading 3.1).

- *Determining the appropriate Atto467N-nanobody dilution for sdTIM*:

  Super-resolution techniques such as Universal Point Accumulation Imaging in Nanoscale Topography (uPAINT) [30, 31], which is ideal for the investigation of plasma membrane protein mobility, require a continuous and stochastic protein labeling at the plasma membrane, using externally applied nanobodies. In contrast, after initial binding to VAMP2-pHluorin at the plasma membrane and following their internalization into synaptic vesicles using sdTIM, the appropriate concentration of the Atto647N-NBs is determined by the balance between the bleaching rate of Atto647N-fluorophores and the renewal of the Atto647N-NBs in the imaging area through the mobility of labeled endocytic structures [21, 22]. In our experience, ideal sdTIM labeling density allows simultaneous tracking of 4 ± 1 recycling synaptic vesicles per presynapse at any given time which can be achieved by preparing a fresh 3.20 pg/µl dilution of anti-GFP Atto647N-NBs in

prewarmed (37 °C) high-K^+ buffer (protect the dilution from light prior to sdTIM experiments) (Subheading 3.6). Note that other fluorescent nanobodies, such as Atto565-labeled nanobodies (Atto565-NBs), can be used at the same concentration for sdTIM. Quantitation of the fluorophore labeling density of the nanobodies (Subheading 3.1), and the number of internalized nanobodies per vesicle (Subheadings 3.8 and 3.9), as well as titrating the nanobody concentration, is highly recommended to ensure optimal imaging conditions, high localization precision (in our studies 36 ± 1 nm for Atto647N-NBs [21] and 32 ± 4 nm for Atto565-NBs [22]), and minimal background when using sdTIM adaptations. Note that ideally the nanobody concentration should be chosen based on presynaptic vesicle labeling density, as the nerve terminals are a far more crowded environment than the axons.

- *Assessment of the number of internalized Atto647N-NBs in fixed neurons*:

  Prepare 4% paraformaldehyde (PFA; e.g., Electron Microscopy Sciences, EMS) in PBS for fixation. Note that PFA is a tissue fixative and should be handled in a fume hood using appropriate protective clothing, gloves, and goggles, and subsequently discarded in accordance with institutional regulations.

2.3 sdTIM Validation and Controls

- *Correlative Light Electron Microscopy (CLEM)*:

  To validate the correct targeting of internalized nanobodies, transfect neurons with VAMP2-pHluorin (using Lipofectamine 2000), and use horseradish peroxidase (HRP)-tagged GFP Nanotrap (HRP-mCherry-GNT) instead of fluorescent nanobodies [22]. For fixation, prepare a fresh solution of 2% glutaraldehyde (e.g., EMS) and 1.5% PFA in PBS pH 7.4. Note that glutaraldehyde is a tissue fixative and must be handled as described above for PFA. For cytochemical staining of the HRP, prepare 1 mg/ml 3,3′-diaminobenzidine tetrahydrochloride (DAB; e.g., Sigma-Aldrich) in PBS, vortex for 5 min, and filter through a 0.2 μm syringe filter. For contrasting, prepare 1% osmium tetroxide (OsO_4) in 0.1 M sodium cacodylate buffer (e.g., Sigma-Aldrich) prior to dehydration and embedding in LX-112 resin (Ladd Research). Note that osmium tetroxide and sodium cacodylate are toxic and should be handled according to the manufacturer's safety instructions and discarded according to institutional regulations.

- *Assessing neuronal maturity and synaptic transmission*:

  For co-transfection (using Lipofectamine 2000), use VAMP2-pHluorin and pmCherry-C1 constructs. Fix with 4% PFA and 4% sucrose (Sigma-Aldrich) in PBS. Permeabilize with 0.1% Triton X-100 (Sigma-Aldrich) in PBS. Blocking solution:

3% goat serum (Gibco) with 0.025% Triton X-100 (Sigma-Aldrich) in PBS. Primary antibody solution: 5% BSA, 1% FBS, and 0.025% Triton X-100 (all from Sigma-Aldrich) in PBS. Secondary antibody solution: 1% goat serum (Gibco) and 0.025% Triton X-100 (Sigma-Aldrich) in PBS. All the washing steps are done with PBS. Mounting: ProLong mounting medium (Thermo Fisher Scientific). Primary antibodies: mouse anti-synapsin-1 and guinea pig anti-MAP2 (both from Synaptic Systems), mouse anti-PSD95 (Abcam), and mouse anti-neurofilament (BioLegend). Secondary antibodies: goat anti-mouse Alexa Fluor 647 and goat anti-guinea pig Alexa Fluor 647 (both from Thermo Fisher Scientific).

2.4 Equipment

- *Neuronal dissection*:

  Laminar flow hood equipped with a dissecting microscope, cell culture incubator at 37 °C with a humidified 5% CO_2, a 37 °C water bath, microcentrifuge, hemocytometer for counting the cells, timer, and a vacuum system for aspiration. Sterile dissecting tools including scissors, forceps, fine-tipped tweezers, and scalpel handle blade. Sterile plasticware including 35 mm glass-bottom cell culture dishes (Cellvis, cat. no. D35-20-1.5N or equivalent), serological pipettes, 60 mm tissue culture dishes, centrifuge tubes, filter tips, disposable filter units (Thermo Fisher Scientific), and glass Pasteur pipettes.

- *Assessment of Atto647N labeling of nanobodies*:

  Glass slides and coverslips (Thermo Fisher Scientific), coverslip tweezers (e.g., Dumont), double-sided tape, compressed air, and a sonicator.

- *Super-resolution microscopy*:

  The method can be implemented on a standard single-molecule microscope operating with oblique illumination. Our super-resolution imaging setup comprises a Roper iLas^2 microscope (Roper Scientific) CFI Apo TIRF, 100×/1.49 NA oil-immersion objective (Nikon) with ×1.5 additional magnification, Piezo Z-drive and Nikon perfect focus system, two electron-multiplying charge-coupled device (EMCCD) cameras (Photometrics), QUAD beam splitter and QUAD band emitter (Semrock), and MetaMorph software for image acquisition (Molecular Devices). Note that other microscopes with a suitable single-molecule detection acquisition rate (here 50 Hz) can be used to implement the sdTIM technique (the requirement for the imaging rate depends on the time scale of the biological phenomenon). For sdTIM setup, we recommend using a custom-made experimental perfusion and aspiration system designed for 35 mm glass-bottom cell culture dishes (for detailed instructions for 3D printing of the custom-made

perfusion lid and construction of the perfusion chamber, *see* [22]) or, alternatively, an equivalent commercially available perfusion system can be used (e.g., PeCon, POC Cell Cultivation System).

- *CLEM*:
  Gridded glass-bottom dishes (P35G-1.5-14-CGRD; MatTek Corporation) and an inverted point-scanning laser confocal microscope (e.g., LMS 510 META, Zeiss) with a Plan-APO 10× 0.45 NA objective (e.g., Zeiss) at 37 °C, argon laser, and Zen 2009 software are used to record the localizations of the VAMP2-pHluorin-positive neurons on gridded dishes. Electron microscopy: BioWave tissue processing system (Pelco), an ultramicrotome (e.g., Leica Biosystems) for thin sectioning, and a transmission electron microscope (e.g., JEOL) equipped with an appropriate camera (e.g., Olympus).
- *Analysis programs*:
  PALMTracer program in MetaMorph [30, 32] or TrackMate plug-in [33] for Fiji/ImageJ (National Institutes of Health) with an additional analysis routine to obtain single-molecule mobility parameters (e.g., MATLAB routine provided in [22]).

3 Methods

3.1 Quantification of the Fluorophore Labeling of the Nanobodies

Nanobodies are emerging as a powerful tool for biological research. The anti-GFP-nanobody, which consists of a variable domain of the heavy chain of HCAbs (V_HH), developed by immunization of a llama [28, 34], has previously been used to track single-glutamate receptors in live neurons [30]. Different fluorophores have different chemical characteristics, and cellular compartments provide varying chemical and physiological environments which can affect the fluorophore brightness, lifetime, and signal-to-noise ratio. We recommend quantifying the fluorophore labeling of the nanobodies (Fig. 2) before performing sdTIM experiments to ensure optimal outcomes.

Due to their small size, high affinity for GFP binding, and a photostable organic fluorophore, anti-GFP Atto647N-NBs are ideal for labeling small endocytic structures such as recycling synaptic vesicles using the sdTIM technique. When studying synaptic vesicle mobility with sdTIM, the externally applied Atto647N-NBs are first exposed to the extracellular space where the pH is typically close to neutral, after which they are internalized into synaptic vesicles where the pH becomes acidic. We therefore recommend the assessment of the Atto647N-NB fluorescence emission to be performed in both neutral (pH 7.0–7.4) and acidic buffers

(pH 5.0–5.5). After the quantification of the labeling density of the nanobodies and following the sdTIM experiments (Subheading 3.6) and single-particle tracking (Subheading 3.7), the number of internalized nanobodies within synaptic vesicles can be quantified (Subheadings 3.8 and 3.9).

1. Quantification of Atto647N-NB labeling density is performed in a purpose-built cell-free flow chamber (note that this can be adapted for the analysis of other fluorophores or probes). Construct the flow chamber by first cleaning the glass slides (22 × 10 × 1 mm) and the rectangular, super-resolution-compatible coverslips by sonication in a glass beaker containing 1 M KOH for 20 min at RT. Wash the glass slides and coverslips with Milli-Q water five times, ensuring that the coverslips do not stick together. Then, dry the glass slides and coverslips individually with a clean airflow. Assemble the flow chamber in a clean environment free of dust, such as a fume hood, by attaching double-sided tape along the length of the glass slide on each side, and align the cleaned rectangular coverslip with the strips of tape by gently pressing the coverslip to create a proper seal and prevent leakage. Handle the cleaned coverslips with tweezers.
2. Pipette the prepared 200 µl of a 3.20 pg/µl dilution of Atto647N-NBs in PBS at pH 7.4 (or pH 5.0, for acidic environment tests) into the flow chamber (*see* **Note 1**) and incubate for 15 min at room temperature (i.e., 22–25 °C) to allow nanobody attachment to the glass surface (*see* **Note 2**). Cover the flow chamber from light to minimize bleaching. Wash the flow chamber twice with PBS pH 7.4 (or pH 5.0 for acidic environment tests) (*see* **Notes 1** and **2**). We recommend avoiding working under direct light as the Atto647N-NBs are light sensitive and performing the recordings without delay to minimize bleaching.
3. Acquire time-lapse images from several regions with oblique illumination (50 Hz, 20-ms exposure, 16,000 frames by image streaming). We recommend to image regions of interest (ROI) that were not exposed to laser illumination prior to image acquisition to prevent bleaching the fluorophores and to allow a reliable estimation of the fluorophore labeling density. This can be done by focusing on an area adjacent to the ROI, then by switching off the laser, and moving to the imaging area without turning the laser on. The laser should be turned on during the first frame or while acquiring the movie. To obtain comparable emission curves, it is important to use the same imaging setup for both cell-free systems and live-cell experiments. Therefore, perform this step at 37 °C. To allow reliable estimation of the fluorophore labeling density, it is important

that the Atto647N-NBs are deposited on the glass surface as separate molecules (*see* **Notes 1** and **2**).

4. To quantify the number of Atto647N fluorophores per nanobody, open obtained images with Fiji/ImageJ software (or any equivalent image analysis program) to analyze the fluorescence emission steps of the Atto647N-NBs. Choose 5 × 5 pixels around the center of each fluorescent spot (to obtain meaningful data, >100 fluorescent spots originating from several regions should be analyzed) to obtain intensity-time traces using the "plot z-axis profile" function in Fiji/ImageJ or, alternatively, a custom-written routine as described previously [35].
5. Subtract the background locally by quantifying the average intensity of a 2 × 2 pixel region surrounding each fluorescent spot. Overlapping nanobodies and fluorophores that bleach within the first two frames of the movies should be excluded from the analysis. Plot fluorescence intensity versus time for all the remaining fluorescent spots. Count the number of emission steps in the intensity-time traces manually (representative intensity-time traces of one and two emission steps are shown in Fig. 2). The mean intensity of the smallest step should be at least twice the standard deviation (SD) of the background fluorescence. The steplike emission traces reflect the bleaching of the Atto674N-fluorophores, and if the Atto647N-NBs are deposited on the glass surface sparsely enough to distinguish separate molecules (for best results, aim for 50–100 Atto647N-NBs per 27 × 27 μm^2), the number of steps will correspond to the number of fluorescent molecules per nanobody (*see* **Notes 1** and **2**).
6. Correct for missed events. In our experience, two molecules of Atto647N-dyes will bleach within the same imaging frame in less than 2% of the traces (these steps are twice the size of single-bleaching steps and should be counted as two). Note that the signal-to-noise ratio should be at least 1.5 to allow accurate assessment of the bleaching steps.

In our preparations of Atto647N-NBs, the average number of Atto647N fluorophores per nanobody is 1.5 [21] indicating that, on average, nanobodies contain either one or two Atto647N fluorophores (Fig. 2). The time course of the fluorescence emission of other fluorescently labeled ligands is determined similarly.

3.2 PLL Coating of Glass-Bottom Cell Culture Dishes

We recommend coating the super-resolution-compatible glass-bottom cell culture dishes (D29-20-1.5N; Cellvis; glass coverslip area 314 mm^2) with PLL at least for 3–4 h. Perform the coating in a sterile fume hood using sterile consumables and reagents.

1. Pipette 300–500 μl of 1 mg/ml PLL in 0.1 M borate buffer pH 8.5 onto the glass surface of the dishes and incubate the dishes at 37 °C at least for 3–4 h.
2. Remove the PLL solution and rinse the coated glass-bottom dish three times with UltraPure DNase/RNase-free dH_2O or sterile PBS pH 7.4. Maintain the coated glass-bottom dish in water until plating the neurons. At this point, the dishes can be stored in a clean, dust-free, area (e.g., in a 4 °C fridge) for several days before use. It is important to avoid drying.

3.3 Hippocampal Neuron Dissections

Rats must be handled according to institutional and governmental ethical guidelines. All reagents and surgical instruments should be sterile. In order to improve the viability of neurons, the procedure must be carried out in ice-cold dissection medium. All experiments should be carried out in accordance with relevant institutional and governmental ethical guidelines and regulations.

1. Following euthanasia by cervical dislocation of a pregnant dam at embryonic days 17–18 (E17–18) (*see* **Note 3**), dissect the uterus, remove the fetuses, and place them in a sterile 60 mm tissue culture dish containing dissection medium. The following steps must be done under a sterile laminar flow cabinet. Using a dissecting microscope, remove the brains and place them in a sterile dish containing dissection medium (Fig. 1). The tissue must remain submerged in the dissection medium at all times.
2. Dissect both forebrains and use fine-tipped tweezers to remove the meninges carefully. Dissect out the hippocampi, gently collect the dissected tissue in an Eppendorf tube, and bring the volume up to 270 μl with dissection medium (Fig. 1). Add 30 μl of 2.5% (wt/vol) trypsin, incubate for 10 min at 37 °C with regular agitation (every 2–3 min), and then stop the trypsinization process by adding 150 μl of FBS (or horse serum) and mixing by tapping the Eppendorf tube. Add 50 μl of 1% (wt/vol) DNase I and incubate for 10 min at 37 °C with regular agitation (every 2–3 min). Then, triturate the tissue by pipetting up and down (40–50 times) using a P200 pipette until the solution is homogenous.
3. Concentrate the cells by centrifugation (120 × *g*, 8 min, at room temperature). Discard the supernatant and resuspend the pellet in 0.5 ml of prewarmed (37 °C) neuronal plating medium. Determine the neuronal density using a hemocytometer and a cell counter and check the cell viability using trypan blue exclusion. We expect 80–90% hippocampal neuron viability, with the number of hippocampal neurons per brain depending on the species (rat or mouse), strain, embryonic

state, and experience of the person performing the dissection. Once isolated, the neurons must be plated as soon as possible as their viability decreases rapidly. Adjust the neuronal density to 50,000–100,000 hippocampal neurons in 0.5 ml of medium.

3.4 Hippocampal Neuron Plating on PLL-Coated Glass-Bottom Cell Culture Dishes

1. Before plating the dissected neurons, aspirate the UltraPure water from the PLL-coated glass-bottom dishes (Subheading 3.2) and rinse the glass-bottom dish once with neuronal plating medium.
2. Aspirate neuronal plating medium and plate the dissected neurons immediately on the glass-bottom dishes (Fig. 1). We recommend doing this step one dish at the time to prevent drying of the PLL-coated glass surface. We use a density of 50,000–100,000 hippocampal neurons in 0.5 ml of medium per 314 mm^2 of the glass surface.
3. Place the neurons in a tissue culture incubator at 37 °C with a humidified 5% CO_2 atmosphere for 2–4 h.

3.5 Hippocampal Neuron Culturing and Transfection

1. Examine culture dishes under a transmission light microscope 2–4 h after plating. Majority of the neurons should be attached to the glass surface, with small filopodia and lamellipodia protruding from the cells [36].
2. Replace the plating medium with 2 ml of neuronal culture medium that can be supplemented with 20% of neuroglial conditioning medium (*see* [22] for further details). Optional: 5 μM Ara-C can be added to the culture dish on DIV3 to decrease the glial cell content (*see* **Note 3**).
3. Every 7 days, refresh the cultures by replacing 1/3 to 1/2 of the medium with fresh neuronal maintenance medium. We recommend performing the sdTIM experiments at DIV14–21 (Fig. 1).
4. Prior to sdTIM, at DIV13–16, transfect the neurons with VAMP2-pHluorin (or another appropriate construct) (Fig. 1). We commonly use Lipofectamine 2000 transfection reagent (other methods can also be used; please *see* **Note 4**) to transfect primary neuron cultures [22, 37]. Pipette 100 μl of room-temperature neurobasal medium into two 1.5 ml Eppendorf tubes. Add 2 μl of Lipofectamine 2000 transfection reagent to one tube and 2 μg of VAMP2-pHluorin to the other tube and mix well by pipetting up and down (we recommend optimization of the total amount and the transfection reagent:plasmid ratio when using other sdTIM adaptations). Incubate the solutions for 5 min at room temperature, and then combine the contents of tubes, mix well, and incubate for 15–30 min at room temperature. Carefully collect the culture medium from the glass-bottom dish in a sterile

tube, leaving a residual volume of 380 µl to cover the neurons in the glass-bottom dish, and pipette the transfection mixture to the neurons in a dropwise manner (only onto the glass-bottom dish). Incubate the neurons for 2–5 h at 37 °C in 5% CO_2 atmosphere. After incubation, remove all excess culture medium from the plastic portion of the dish, wash the neurons 3–5 times gently with fresh prewarmed (37 °C) neurobasal medium, and then replace the medium with the medium collected from the glass-bottom dishes prior to the transfection (make sure that the collected culture medium is prewarmed at 37 °C). Continue transfection of the neurons for 24–48 h.

3.6 sdTIM: Induction of Synaptic Activity and Internalization of Atto647N-NBs into Recycling Synaptic Vesicles

Induction of synaptic activity and uptake of Atto647N-NBs (Fig. 3a) in DIV14–21 hippocampal neurons expressing VAMP2-pHluorin (Fig. 3b) can be done in glass-bottom dishes equipped with a custom-made perfusion lid (details of the 3D printing can be found in ref. 22), which allows a gentler exchange of liquid compared to pipetting straight onto the neurons and allows the liquid exchange at the microscope without having to remove the dish from the dish holder. Using the perfusion lid allows liquid exchange on the plastic-bottom surface of the cell culture dish, leaving the glass-bottom portion of the dish submerged (remnant volume ~380 µl) at all times, which protects the neurons from drying. We recommend taking into account the remaining volume in the glass bottom of the dish when calculating the nanobody dilutions. To induce synaptic activity and internalization of Atto647N-NBs into recycling synaptic vesicles, follow the steps below:

1. Prewarm the low-K^+ and high-K^+ buffers to 37 °C, prepare a 3.20 pg/µl dilution of anti-GFP Atto647N-NBs in prewarmed high-K^+ buffer, and cover it from light.
2. Remove the culture medium by aspiration and gently wash the neurons 4–5 times with 2 ml of prewarmed low-K^+ buffer (Fig. 3a). Immediately transfer the dish to the microscope and replace the culture dish lid with the perfusion lid. Attach two syringes to the perfusion lid tubing: an empty 10 ml syringe for aspiration and another 10 ml syringe filled with 2 ml of prewarmed high-K^+ buffer containing 3.20 pg/µl of Atto647N-NBs for the injection. Protect the Atto647N-NB solution from light using foil. Optional step: We recommend adding fluorescent beads diluted in low-K^+ buffer during the last washing step to augment drift correction (*see* **Note 5**).
3. Locate a representative hippocampal neuron expressing VAMP2-pHluorin (Fig. 3b) (*see* **Note 4**). Aspirate the low-K^+ buffer from the dish carefully (removed volume ~1.6 ml), leaving the glass-bottom portion of the dish submerged in the

low-K^+ buffer. Then, add the high-K^+ buffer containing 3.20 pg/μl of Atto647N-NBs to the dish to induce synaptic activity while simultaneously recording the unquenching of the VAMP2-pHluorin fluorescence (Fig. 3b, c; *see* **Note 5**). Acquire images at 50 Hz and 20-ms exposure time over 3000–5000 frames and stimulate the neurons for 5 min in total at 37 °C without removing the plate from the microscope (Fig. 3b). Alternatively, record a short movie or take a snapshot of VAMP2-pHluorin fluorescence prior to and immediately after stimulation, to compare the VAMP2-pHluorin mean fluorescence intensity (MFI) before and after the pulse. This will provide adequate information to identify active presynapses. As the unquenching of VAMP2-pHluorin fluorescence occurs quickly after the stimulation, the imaging should therefore be done immediately.

4. After 5-min stimulation, aspirate the high-K^+ buffer from the dish (remove ~1.6 ml) and carefully inject 2 ml of prewarmed low K^+ into the dish. Repeat this step five times to remove any traces of unbound Atto647N-NBs and incubate the plate for 10 min (chase) in total (Fig. 3a) (*see* **Notes 5** and **6**).
5. After the 10-min chase, acquire time-lapse images of the VAMP2-pHluorin-bound Atto647N-NBs internalized into recycling synaptic vesicles with oblique illumination microscopy (Fig. 3a) (50 Hz, 20-ms exposure, 16,000 frames by image streaming) using the same microscope settings as described in **step 5** of Subheading 3.1 (*see* **Notes 5** and **6**). The imaging should be done in the same ROI in which the VAMP2-pHluorin fluorescence was recorded (**step 3** of Subheading 3.6) (Fig. 3b) to correlate the single-molecule acquisition to VAMP2-pHluorin fluorescence information (Fig. 3d).
6. Proceed with single-molecule tracking (Subheading 3.7).

3.7 Single-Molecule Tracking with TrackMate

Different software packages are available for single-molecule detection and tracking [38]. The PALM-Tracer software [30, 32] operating in the MetaMorph software, which is used in our laboratory, employs a combination of wavelet segmentation [39] and optimization of multiframe object correspondence by simulated annealing [40], and allows single-molecule tracking. Alternatively, freely available software packages can be used for single-molecule tracking. Below we describe a single-molecule detection and tracking routine using TrackMate software [33] in conjunction with an additional analysis routine in MATLAB [22], which computes mean-square displacement (MSD) and diffusion coefficients (available for download at [22]).

1. Open the time-lapse acquisitions of internalized Atto647N-NBs (Subheading 3.6) using TrackMate software. If desired, a

presynaptic and axonal segment ROIs can be drawn at this stage.

2. Run TrackMate plug-in (select the "LoG detector," "median filter," and "subpixel localization" in the particle detection process). Adjust the linking distance, which depends on the time resolution and mobility of fluorescent spots, in the Simple LAP tracker while keeping the gap closing at zero to link single-particle mobility into tracks. We recommend choosing an exposure time which prevents the Atto647N-NBs from moving distances greater than the diameter of the point spread function of the microscope between adjacent frames of the acquisition. Then, run the tracker.
3. Select particle traces as appropriate using the spot-filtering options of the TrackMate. Generate the "Spots in Tracks Statistics" text file containing the x and y coordinates, as well as the spot intensity values, of the fluorescent spots linked into each track.
4. A custom-written MATLAB code and detailed instructions on how to use the scripts are available to download from [22]. Presynaptic and axonal ROIs can be manually selected before the tracking, which allows the discrimination of single-particle tracks of synaptic vesicles originating from these distinct regions [21] (active presynapses can be discriminated from axons by following the acquired VAMP2-pHluorin fluorescence videos obtained in Subheading 3.6; Fig. 3b, c). Run the downloaded MATLAB routine to compute the mean square displacement (MSD) curves and diffusion coefficients.

Here, using in silico simulations, we show the expected MSD curves of particles undergoing Brownian, directed, or confined motion (Fig. 4a, b). To validate the sdTIM technique [21], single-molecule mobility of VAMP2-pHluorin-bound Atto647N-NBs internalized in recycling synaptic vesicles in live hippocampal neurons was compared to that of those transiting on the plasma membrane using uPAINT technique [30, 31] (Fig. 5). Our results showed that the mobility of VAMP2-pHluorin-bound Atto647N-NBs internalized in recycling synaptic vesicle pool (imaging using sdTIM) differs significantly from the mobility of those located on the plasma membrane (imaging using uPAINT) [21].

Recycling synaptic vesicles switch stochastically between distinct motion states [21]. Here, the MSD and distribution of diffusion coefficients of particles switching between two distinct diffusive states are shown (Fig. 6) using MCell tool simulation [41]. By applying Bayesian model selection applied to hidden Markov modeling (HMM-Bayes), we investigated the anomalous and

subdiffusive events of recycling synaptic vesicle mobility in live hippocampal neurons, and discovered that, in most nerve terminals, SVs stochastically switch between purely diffusive (D) and transport mobility (DV) states (Fig. 7) [21].

3.8 Procedure to Quantify the Number of Internalized Nanobodies Within Recycling Synaptic Vesicles in Fixed Neurons

Ideally, only one anti-GFP nanobody with a single Atto647N-tag would get internalized into an individual synaptic vesicle. Since VAMP2 is an abundant synaptic SNARE protein and, on average, up to 70 copies of VAMP2 can be found in a synaptic vesicle [42], with significant intervesicular variability [43, 44], it is possible that more than one Atto647N-NB may get trapped in a single synaptic vesicle, even when used at very low concentrations. To quantify the number of internalized VAMP2-pHluorin-bound Atto647N-NBs in fixed neurons, follow the steps below, and then continue to Subheading 3.9 to quantify the number of internalized VAMP2-pHluorin-bound Atto647N-NBs in live neurons.

1. Fix the neurons with freshly prepared 4% (wt/vol) PFA in PBS for 20 min in a fume hood following the 10-min chase in sdTIM (Subheading 3.6). Wash the neurons three times with PBS, leaving the sample covered in PBS. Continue with imaging without delay.
2. Image the internalized Atto647N-NBs using oblique illumination microscopy as described in Subheading 3.6.
3. Calculate the fluorescence emission steps of internalized Atto647N-NBs in fixed neurons by opening the time-lapse movies in ImageJ software and following the instructions in Subheading 3.1. Internalized VAMP2-pHluorin-bound Atto647N-NBs in synaptic vesicles will exhibit a similar steplike emission to that observed in the cell-free flow chamber experiments (Fig. 2a; Subheading 3.1). Calculate the number of emission steps originating from single synaptic vesicles manually as outlined in Subheading 3.1. Continue with quantification of the number of internalized Atto647N-NBs in recycling synaptic vesicles in live hippocampal neurons (Subheading 3.9).

Reflecting the number of Atto647N fluorophores internalized within synaptic vesicles, in our experiments the average number of emission steps originating from single synaptic vesicles is 1.5 (ranging from one to three), with the majority of synaptic vesicles exhibiting a single emission step [21]. Based on these quantifications, the majority of synaptic vesicles contain a single internalized Atto647N-NB with either one or two Atto647N fluorophores attached to it.

3.9 Procedure to Quantify the Number of Internalized Nanobodies Within Recycling Synaptic Vesicles in Live Neurons

To quantify the number of internalized VAMP2-pHluorin-bound Atto647N-NBs in live neurons, follow the steps below:

1. Following the 10-min chase in sdTIM, image internalized VAMP2-pHluorin-bound anti-GFP Atto647N-NBs in live neurons using oblique illumination microscopy as described in Subheading 3.6.
2. To determine the number of synaptic vesicles that reside within the nerve terminal at any given time, two methods can be used (*see* **steps 3** and **4**).
3. In the first approach, open the acquired time-lapse movies in ImageJ software and choose an ROI to cover the whole presynaptic terminal (presynapses can be discriminated from adjacent axonal segments based on the round morphology of the bouton and the VAMP2-pHluorin unquenching), and measure the Atto647N-NB fluorescence intensity over time as described in Subheading 3.1. The internalized Atto647N-NBs exhibit similar steplike emission to that in fixed neurons, with the number of steps reflecting the number of Atto647N fluorophores within that region. The average number of emission steps in presynapses is 6.0 ± 1.6 (SD) in our experiments [21].
4. In the second approach, record the fluorescence intensity of each internalized Atto647N-NB along its trajectories. This can be done after the single-molecule tracking of VAMP2-pHluorin-bound anti-GFP Atto647N-NBs in live neurons (Subheading 3.7). Open the "Spots in Tracks Statistics" text file containing the fluorescence intensity assigned to each spot in a track. Plot the fluorescence intensity assigned to each spot against time and count the number of observed steps. The Atto647N-NB fluorescence level along the trajectories remains unchanged until either the Atto647N-NB bleaches and the fluorescence intensity trace drops to the background level or a second recycling synaptic vesicle enters the same diffraction-limited presynaptic ROI causing a steplike increase in fluorescence. The total number of emission steps from the trajectories within the same presynapse (5.4 ± 1.3 on average in our experiments [21]) reflects the number of Atto647N fluorophores within that region and should be similar to the quantification results in **step 3**.
5. The number of simultaneously detected synaptic vesicles in presynapses at any given time can then be estimated from the number of Atto647N fluorophores per nanobody (Subheading 3.1), the number of internalized Atto647N-NBs per synaptic vesicle (Subheading 3.8), and the number of fluorescence emission steps in the presynapses (above).

In our experiments, the number of synaptic vesicles we can detect at any given time within a presynapse, by tracking VAMP2-pHluorin-bound anti-GFP Atto647N-NBs, is 4 ± 1 [21].

3.10 sdTIM Validation and Controls

3.10.1 CLEM

The activity-dependent internalization of the anti-GFP Atto647N-NBs depends on their binding to VAMP2-pHluorin. Although Atto647N-NBs exhibit high affinity to GFP, and are therefore likely to enter solely into VAMP2-pHluorin-expressing cells, the following points may need to be considered when performing sdTIM experiments: (1) overexpression of any construct may cause mislocalization artifacts, (2) bulk endocytosis contributes to compensatory endocytosis of recycling synaptic vesicles [45], and (3) nanobodies may get internalized in endocytic structures other than synaptic vesicles, such as endosomes, even when used at a very low concentration. To assess the correct localization of the internalized nanobodies in synaptic vesicles we performed CLEM as follows:

1. Grow hippocampal neurons from rats (E18) on PLL-coated (Subheading 3.1) gridded glass-bottom dishes (P35G-1.5-14-CGRD-D; MatTek Corporation; 154 mm^2 glass coverslip area) and transfect with VAMP2-pHluorin on DIV14–16 for 24–48 h (Fig. 8a, b). We use a density of 25,000–50,000 hippocampal neurons per 154 mm^2 of the glass surface. These specialized dishes have alphanumeric location markers etched into the glass coverslip in the bottom of the dish, allowing the correlation of light and electron microscopy images.
2. On DIV15–17, image the neurons live at 37 °C with an appropriate fluorescence microscope (such as on an inverted point-scanning laser confocal microscope, LSM 510 Meta, Zeiss) to record the location of VAMP2-pHluorin-positive neurons (Fig. 8a) on the cover grids (Fig. 8b).
3. Process the neurons for sdTIM as described in Subheading 3.6, except for using HRP-mCherry-GNT nanobodies instead of Atto647N-NBs. Omitting the live-cell imaging of the synaptic vesicles is optional.
4. Fix the neurons with 2% glutaraldehyde and 1.5% PFA in PBS for 1 h at room temperature.
5. Quench the free aldehyde groups with 20 mM glycine in PBS for 20 min at room temperature, and then wash the neurons with PBS.
6. For cytochemical staining, prepare 1 mg/ml DAB in PBS, add 1 ml of this equilibration buffer to each dish, and incubate for 5 min at room temperature. Add 3 μl of 30% H_2O_2 to 5 ml of 1 mg/ml DAB in PBS to prepare the reaction buffer and protect the tube from light as the solution is very light sensitive.

Replace the DAB equilibration buffer in each dish with 1 ml DAB reaction buffer and incubate in the dark for 20 min at room temperature. Wash 3 × 5 min with PBS.

7. Osmicate with 1% OsO_4 (aq) in 0.1 M sodium cacodylate buffer using the following settings: 80 W Vac ON for 2 min ON, 2 min OFF, and 2 min ON (performed in the Pelco BioWave). Repeat this step without a solution change, then remove the osmium, and rinse with Milli-Q water.
8. Replace the Milli-Q water and place the cell culture dish in the BioWave using 80 W Vac OFF for 40 s.
9. Dehydration series are performed in the BioWave as follows: Remove water and replace with 50% EtOH using 250 W Vac OFF for 40 s. Repeat using 70% and 90% EtOH ones and 100% EtOH twice.
10. Perform resin infiltration using LX112 resin. Prepare 33%, 50%, 66%, and 100% LX112 in 100% EtOH. Incubate cells in the BioWave in 33% LX112 resin using 250 W and Vac ON for 3 min. Repeat using 50% and 66% resin once and 100% resin twice.
11. Ensure that only a thin film of resin is left on the glass bottom of the dishes and polymerize the resin in a 60 °C oven for 24 h.
12. After polymerization, remove the dish from the oven and detach the polymerized block from the dish by plunging the disk into liquid nitrogen for 15–20 s. Use a razor blade to pry the plastic and glass away from the resin (additional liquid nitrogen immersion may be used if the resin does not detach easily).
13. Once the resin is separated, the imprinted grid squares from the dish will be visible as an impression on the resin. This is the monolayer where the cells reside. Using pliers, cut away the sides of the dish and all the corners until just a flat disk of resin and dish remains.
14. Identify the ROI using a dissecting microscope to view the grid squares. The correct location can be found using the fluorescence and phase-contrast images recorded earlier (**step 2**). Circle the grid squares of interest with a fine-tip sharpie. Use pliers and a fine-tooth saw to cut the individual grid squares (~3 grid squares may be isolated provided that they are not too close to one another).
15. Paying close attention to orientation, stick the resin grid squares to blank resin blocks that have been roughened up with wet and dry sandpaper. Use LX112 or Epon as the adhesive rather than super glue which may obscure the alphanumeric locators on the grid squares if applied too generously. Incubate the blocks in the 60 °C oven for 16 h.

16. When making a block face for sectioning, a nonsymmetrical shape should be trimmed to correspond to a particular area identified by fluorescence microscopy so that the electron micrographs can be aligned with the fluorescence data; once the sections are cut for electron microscopy the only points of registration will be the shape of the section as fluorescence data and the grid square identifiers will no longer be visible.
17. Flip the fluorescence image horizontally and print it. Once on the transmission electron microscope, the distribution of cells seen on this printout will provide the pattern to identify the same distribution of cells on the phosphor screen. When that pattern is identified, the VAMP2-pHluorin-positive cells can be located and imaged, and the localization of the internalized anti-GFP HRP-mCherry-GNT nanobodies can be assessed based on the electron-dense HRP precipitate (Fig. 8c).

Our results showed that HRP precipitate was only detected in neurons expressing VAMP2-pHluorin, indicating that HRP-mCherry-GNT binds specifically only to VAMP2-pHluorin [21]. In neurons expressing VAMP2-pHluorin, a great majority ($88.5 \pm 3.0\%$) of the HRP precipitate was found in recycling synaptic vesicles, while some residual staining was detected on the plasma membrane and in endocytic structures larger than 45 nm in diameter [21]. These results provide support to the activity-dependent internalization of the anti-GFP nanobodies into recycling synaptic vesicles.

3.10.2 Assessing Neuronal Maturity

In order to ensure the imaging of vesicles in functional synapses, it is essential to perform the sdTIM experiments in mature neurons. We recommend a combination of different morphological features and neuronal markers to assess the maturity of the hippocampal neurons. The simultaneous co-transfection with VAMP2-pHluorin and an empty vector (here, pmCherry-C1) will facilitate the analysis of the distribution of overexpressed VAMP2, allowing the simultaneous determination of the maturity state. Mature neurons show prominent spines along the dendritic arbor [46] (Fig. 8d, f) and axonal enlargements corresponding to synaptic boutons [47] (Fig. 8e). VAMP2-pHluorin is distributed along the neuronal soma and the axon, colocalizing with the axonal marker neurofilament (Fig. 8d) and to a lesser extent with microtubule-associated protein 2 (MAP2; Fig. 8f). VAMP2-pHluorin is expressed in presynaptic boutons together with another synaptic vesicle protein, synapsin-1 (Fig. 8e), forming connections with dendritic spines, here stained with postsynaptic density protein 95 (PSD95; Fig. 8g). To assess the maturity of hippocampal neurons, perform immunofluorescence assay as follows:

1. Grow hippocampal neurons from rats (E18) on PLL-coated (Subheading 3.2) glass-bottom dishes and co-transfect the

neurons with VAMP2-pHluorin and pmCherry-C1 on DIV14–16 for 24–72 h.

2. At DIV15–19, aspirate the neuronal medium and wash the neurons with PBS to remove dead cells and cell debris. In the following steps, as the neurons express VAMP2-pHluorin, it is important to protect the specimen from light by performing all the incubation in a dark box. It is also critical to ensure that the dishes never dry as this will damage the complex neuronal architecture.
3. Fix the neurons with PBS-PFA-sucrose for 15 min at room temperature.
4. Wash the samples three times with PBS.
5. Permeabilize the neurons with PBS-Triton X-100 for 10 min at room temperature.
6. Wash the samples once with PBS.
7. Perform the blocking step by incubating the neurons with blocking solution for 1 h at room temperature.
8. Wash the samples three times with PBS.
9. Incubate the neurons with appropriate primary antibodies for 3 h at room temperature or overnight at 4 °C. Due to the duration of this step, it is highly recommended that a humid chamber be created using soaked tissue to prevent evaporation of the antibody solution.
10. Wash the samples 3–5 times, 5 min each, with PBS.
11. Incubate the neurons with appropriate secondary antibodies for 1 h at room temperature.
12. Wash the samples 3–5 times, 5 min each, with PBS.
13. Mount the samples. Once the mounting medium is dry, the neurons are ready for imaging. We currently use an inverted point-scanning laser confocal microscope (LSM 510 Meta, Zeiss). The prepared samples can be stored for several weeks to months, protected from light, at 4 °C.

3.10.3 Monitoring Neuronal Secretion and Synaptic Transmission with a pH-Sensitive Fluorophore

Transfecting hippocampal neurons with VAMP2-pHluorin (other potential recycling synaptic vesicle protein targets are discussed in Subheading 3.11) is important to implement the sdTIM technique for the study of synaptic vesicle recycling. pH-sensitive indicators (such as pHluorin [23, 24]) can also be used to discriminate active presynapses from the adjacent axonal segments [21, 22]. Synaptic vesicles fuse with the plasma membrane in response to high K^+ stimulation, exposing VAMP2-pHluorin to the extracellular space and leading to fluorescence intensity increases in presynaptic sites of secretion (Fig. 3b), thereby confirming synaptic transmission [11, 21, 22].

3.11 Potential sdTIM Adaptations

The pulse-chase-based sdTIM technique can be relatively easily adapted to study any endocytic structure in various cell types. We first used sdTIM to investigate the role of presynaptic activity in the retrograde transport of autophagosomes (from the nerve terminal to the cell soma) using externally applied botulinum neurotoxin type-A (BoNT/A) [3]. Although autophagosomes can be imaged with conventional light microscopy, the detection of a very low concentration of BoNT/A in autophagosomes can only be achieved with single-molecule super-resolution microscopy, as only a few molecules are likely to enter each retrograde carrier. We then used sdTIM to localize retrogradely transported signaling endosomes in axons labeled with Alexa Fluor 647-conjugated cholera toxin subunit-B (Alexa647-CTB), using structured illumination microscopy (SIM) [2]. Most recently, we have used sdTIM to image recycling synaptic vesicles in their natural crowded presynaptic environment [21] and we have demonstrated the successful use of sdTIM technique for dual-color imaging of synaptic vesicles, using anti-GFP Atto565-NBs, in conjunction with signaling endosomes, using Alexa647-CTB [22], thereby opening a path for multicolor super-resolution imaging of different subdiffractional cellular structures. The current pulse-chase configuration of the sdTIM protocol (i.e. 5-min stimulation and 10-min chase) mainly labels the dynamic pool of synaptic vesicles, known as the recycling pool (the other two major pools being the readily releasable pool and the reserve pool; the classical and emerging roles of synaptic vesicle pools are reviewed in [48]). By adjusting the pulse (and hence the strength of the stimulus), the chase duration, and the timing of Atto647N-NB (or other) application or by reintroducing a second stimulus after the Atto746N-NB internalization, other synaptic vesicle pools can potentially be studied with sdTIM. Alternatively, evoked synaptic activity could be studied by combining sdTIM with electric field stimulation systems [49]. The mobility of inter-bouton synaptic vesicles, which form the so-called exchange or super-pool of synaptic vesicles, can also be studied based on the morphological information about the neuron by region-specific analysis of synaptic vesicles. The surface pool (i.e., synaptic vesicles following fusion with the plasma membrane) [21] can be studied with uPAINT [30, 31].

There are multiple potential adaptations of the sdTIM configuration to image cell endocytic pathways and cargo trafficking. Other potential synaptic vesicle markers such as synaptobrevins (Syb or VAMP) [50, 51], synaptotagmins (Syt) [52, 53], synaptophysins (SypHy) [52–54], vesicular glutamate transporter 1 (vGlut1) [52, 55], Vps10p-tail-interactor-1a (vti1a) [56] and synaptic vesicle 2 (SV2) [52, 53], and V-type ATPase [52], that can be tagged with a pHluorin moiety in the vesicle lumen, could potentially be used instead of VAMP2. Other fluorophores, such as

RFP, can also be used when employing anti-RFP nanobodies (commercially available from Synaptic Systems). sdTIM can also be combined with sptPALM to image fluorescently labeled endocytic cargoes in conjunction with intra- or extracellular overexpressed mEos-tagged (or analogue) proteins, thereby expanding the use of the sdTIM technique. In addition to adaptations to follow the internalization of other synaptic vesicle proteins or different plasma membrane proteins destined for endocytosis, sdTIM can potentially be adapted to study different endocytic cargoes (e.g., neurotropic factors, monoclonal antibodies, cell-penetrating peptides used for drug delivery), toxins (e.g., cholera and botulinum toxins [2, 3, 29, 57–59]), cellular endocytic and membrane-trafficking regulators (e.g., Rab- and Rho-GTPases), and pathogen internalization (e.g., poliovirus) [22].

We have also used sdTIM to study neurons cultured on custom-made microfluidic devices (for detailed instructions regarding the microfabrication, *see* [22]), which allows polarized culturing of neurons. Microfluidic devices expand the potential use of the sdTIM technique even further by enabling (i) region-specific application of pharmacological agents to the cell culture dish; (ii) transfection of the microfluidic soma and terminal wells with, e.g., pre- and postsynaptic markers, to study synaptic connections; and (iii) the study of other cell–cell connections, such as neuromuscular junctions, by culturing muscle cells and neurons in the microfluidic soma and terminal wells, respectively.

4 Notes

1. *Separate Atto647N-NBs cannot be discriminated in the flow chamber*:

   If the density of nanobodies on the glass surface is too high to discriminate single molecules (Subheading 3.1), this may be due to the concentration of the Atto647N-NBs being too high or insufficient washing. Wash the flow chamber again with PBS to remove excess Atto647N-NBs or prepare a higher dilution of Atto647N-NBs and repeat Subheading 3.1. Note that while a brief exposure to far-red laser can be used to bleach a subset of internalized nanobodies in live neurons (*see* **Note 6**), we do not recommend a similar step for the flow chamber system. Exposure to far-red laser prior to acquisition will preclude the quantitation of fluorophore labeling of the nanobodies.

2. *Atto647N-NBs move in the flow chamber during imaging*:

   This may indicate that the incubation time was too short to allow proper attachment to the glass surface. Allow a longer

incubation time and perform the washing steps gently (Subheading 3.5).

3. *Glial content on the cell culture dish is too high*:
   Use E18 embryos instead of postnatal pups (Subheading 3.3). The neuronal culture medium can be supplemented with 5 μM Ara-C on DIV3 to decrease the glial content (Subheading 3.5).
4. *Low transfection efficiency*:
   Primary neurons are challenging to transfect (Subheading 3.4). We usually obtain a better transfection efficiency with younger cultured neurons (i.e., DIV14–16 or younger) than those that are more mature (i.e., >DIV16) using Lipofectamine 2000 transfection reagent. Note that some optimization may be required when using different expression constructs and/or transfection reagents. If the transfection efficiency is very low, consider transfecting younger neuronal cultures, changing the transfection time, and/or adjusting the DNA concentration of the transfection reaction mix. Note that if the duration of the transfection is prolonged, additional controls for possible overexpression artifacts may be required. When creating the transfection mixture, it is important to use neurobasal medium without any supplements, especially antibiotics, which will decrease the transfection efficiency. When performing the transfection, it is very important to never remove all the medium from the neurons, which may decrease the viability of the neurons. Prior to pipetting the transfection mix to the neurons, collect the culture medium from the plastic surface, leaving some residual medium (~380 μl) in the glass-bottom part to cover the neurons. It is very important to remove all transfection reagent from the plates after the incubation, to avoid cell death, by performing 3–5 washing steps. Alternatively, other transfection methods such as calcium phosphate transfection [60] or nucleofection [61] prior to plating the neurons can be used.
5. *The region of interest is lost during high-K^+ stimulation or low-K^+ washes*:
   We recommend using the perfusion system to carry out the sdTIM protocol (Subheading 3.6), as it does not require removing the plate from the microscope in between the protocol steps and allows a gentler liquid exchange on the plate to decrease possible drift issues. If the ROI is lost during the injection or aspiration of liquids, use less syringe pressure. If the neurons react to stimulation by moving, check that the high-K^+ buffer is made correctly, has the right pH and osmolarity, and is at the correct temperature. Image drift during the acquisition can be corrected using the fluorescent beads

(Subheading 3.6, **step 2**) and an appropriate software (e.g., PALMTracer program in MetaMorph [30, 32] or MIB [62].

6. *The concentration of Atto647N-NBs in the culture dish is too high, so that single synaptic vesicles cannot be discriminated*:

   The sdTIM technique is based on the uptake of externally applied Atto647N-NBs, followed by imaging with oblique illumination microscopy to detect only the bound Atto647N-NBs with minimal background. We stress that the concentration of the fluorescent probe must be titrated to allow optimal labeling of the endocytic structure of interest. For example, aiming for optimal labeling of synaptic vesicles in the highly crowded presynaptic environment, compared to in the adjacent axons, is a limiting factor. In our experience, ideal labeling density allows simultaneous tracking of 4 ± 1 recycling synaptic vesicles in a presynapse at any given time [21]. If single recycling synaptic vesicles cannot be discriminated on the plate and single molecules overlap, the washing steps may have been insufficient (Subheading 3.6) or the concentration of the Atto647N-NBs was too high. We recommend repeating Subheading 3.5 with a fresh neuronal culture, as well as increasing the number of washes with an adequate volume after the high-K^+ stimulation and decreasing the concentration of the Atto647N-NBs on the dish. Alternatively, the nerve terminals can be briefly exposed to far-red laser illumination to bleach some of the fluorophores (optional).

5 Conclusions

Understanding the molecular mechanisms underpinning synaptic vesicle release and recycling is an important aspect of modern neurobiology [63–66]. Traditionally, only electrophysiology, indirect fluorescent recovery after photobleaching (FRAP), and electron microscopy have allowed the study of synaptic vesicle recycling. Assessing the nanoscale synaptic environment and the mobility of individual synaptic vesicles is a powerful strategy to study presynaptic functions, synaptic connections, and neurotransmission. Super-resolution imaging techniques are essential to achieving such in-depth knowledge on the key molecular step of information transfer and storage. sdTIM is a recently developed localization microscopy-based super-resolution technique that allows the study of the recycling and exchange pools of synaptic vesicles, or other endocytic structures, with high spatiotemporal resolution (here, 20-ms time resolution and 30–40 nm localization precision for synaptic vesicles using Atto647N-NBs) [21, 22]. The main advantage of this technique is the production of a high density of trajectories for each presynapse, reaching the thousands for each

neuron, thereby enabling the identification of discrete diffusive states. Importantly, this in turn allows hidden mobility parameters to be investigated, such as the number of distinct diffusional and transport states and switching between them, by applying hidden Markov models (HMMs) and Bayesian model selection (HMM-Bayes) to the sdTIM data [67, 68]. By employing HMM-Bayes to study synaptic vesicle mobility, we were able to annotate mobility along synaptic vesicle trajectories and discovered that, in most nerve terminals, recycling synaptic vesicles stochastically switch between purely diffusive and transport mobility states, and are relatively less likely to switch from diffusive states to transport states in either resting or stimulated neurons [21, 22]. The quantitative account of the heterogeneous nature of synaptic vesicle mobility in live presynapses demonstrated that the commonly used bulk measurements for the description of synaptic vesicle mobility provide only a limited view of the dynamic signature of synaptic vesicles.

Acknowledgments

The super-resolution imaging was carried out at the Queensland Brain Institute's (QBI) Advanced Microimaging and Analysis Facility. We thank all the authors of the original studies for their contribution [21, 22], and our collaborators for helpful discussions, and we would like to further extend our gratitude to N. Valmas for the schematic illustrations presented here, R. Amor for technical support on imaging, I. Morrow for support on EM, and R. Tweedale (QBI) for critical appraisal of the chapter. This work was supported by an Australian Research Council Discovery Project grant (DP150100539), an Australian Research Council Linkage Infrastructure, Equipment, and Facilities grant (LE130100078), and a National Health and Medical Research Council (NHMRC) grant (1120381) to F.A.M. M.J. is supported by an Academy of Finland Postdoctoral Research Fellowship (298124). F.A.M. is a NHMRC Senior Research Fellow (1060075).

References

1. Denker A et al (2011) A small pool of vesicles maintains synaptic activity in vivo. Proc Natl Acad Sci U S A 108(41):17177–17182
2. Wang T et al (2016) Flux of signalling endosomes undergoing axonal retrograde transport is encoded by presynaptic activity and TrkB. Nat Commun 7:12976
3. Wang T et al (2015) Control of autophagosome axonal retrograde flux by presynaptic activity unveiled using botulinum neurotoxin type a. J Neurosci 35(15):6179–6194
4. Fowler MW, Staras K (2015) Synaptic vesicle pools: principles, properties and limitations. Exp Cell Res 335(2):150–156
5. Denker A, Rizzoli SO (2010) Synaptic vesicle pools: an update. Front Synaptic Neurosci 2:135
6. Rizzoli SO, Betz WJ (2005) Synaptic vesicle pools. Nat Rev Neurosci 6(1):57–69

7. Chamberland S, Toth K (2016) Functionally heterogeneous synaptic vesicle pools support diverse synaptic signalling. J Physiol 594 (4):825–835
8. Alabi AA, Tsien RW (2012) Synaptic vesicle pools and dynamics. Cold Spring Harb Perspect Biol 4(8):a013680
9. Crawford DC, Kavalali ET (2015) Molecular underpinnings of synaptic vesicle pool heterogeneity. Traffic 16(4):338–364
10. Kamin D et al (2010) High- and low-mobility stages in the synaptic vesicle cycle. Biophys J 99 (2):675–684
11. Gimber N et al (2015) Diffusional spread and confinement of newly exocytosed synaptic vesicle proteins. Nat Commun 6:8392
12. Hua Y et al (2011) A readily retrievable pool of synaptic vesicles. Nat Neurosci 14(7):833–839
13. Willig KI et al (2006) STED microscopy reveals that synaptotagmin remains clustered after synaptic vesicle exocytosis. Nature 440 (7086):935–939
14. Hu Y, Qu L, Schikorski T (2008) Mean synaptic vesicle size varies among individual excitatory hippocampal synapses. Synapse 62 (12):953–957
15. Lemke EA, Klingauf J (2005) Single synaptic vesicle tracking in individual hippocampal boutons at rest and during synaptic activity. J Neurosci 25(47):11034–11044
16. Westphal V et al (2008) Video-rate far-field optical nanoscopy dissects synaptic vesicle movement. Science 320(5873):246–249
17. Hoopmann P et al (2010) Endosomal sorting of readily releasable synaptic vesicles. Proc Natl Acad Sci U S A 107(44):19055–19060
18. Lehmann M et al (2015) Multicolor caged dSTORM resolves the ultrastructure of synaptic vesicles in the brain. Angew Chem Int Ed Engl 54(45):13230–13235
19. Maschi D, Klyachko VA (2017) Spatiotemporal regulation of synaptic vesicle fusion sites in central synapses. Neuron 94(1):65–73.e3
20. Peng A et al (2012) Differential motion dynamics of synaptic vesicles undergoing spontaneous and activity-evoked endocytosis. Neuron 73(6):1108–1115
21. Joensuu M et al (2016) Subdiffractional tracking of internalized molecules reveals heterogeneous motion states of synaptic vesicles. J Cell Biol 215(2):277–292
22. Joensuu M et al (2017) Visualizing endocytic recycling and trafficking in live neurons by subdiffractional tracking of internalized molecules. Nat Protoc 12(12):2590–2622
23. Miesenbock G, De Angelis DA, Rothman JE (1998) Visualizing secretion and synaptic transmission with pH-sensitive green fluorescent proteins. Nature 394(6689):192–195
24. Royle SJ et al (2008) Imaging phluorin-based probes at hippocampal synapses. Methods Mol Biol 457:293–303
25. Villarreal S, Lee SH, Wu LG (2017) Measuring synaptic vesicle endocytosis in cultured hippocampal neurons. J Vis Exp (127)
26. Fiolka R (2016) Clearer view for TIRF and oblique illumination microscopy. Opt Express 24(26):29556–29567
27. Giannone G et al (2010) Dynamic superresolution imaging of endogenous proteins on living cells at ultra-high density. Biophys J 99 (4):1303–1310
28. Rothbauer U et al (2006) Targeting and tracing antigens in live cells with fluorescent nanobodies. Nat Methods 3(11):887–889
29. Harper CB et al (2016) Botulinum neurotoxin type-A enters a non-recycling pool of synaptic vesicles. Sci Rep 6:19654
30. Nair D et al (2013) Super-resolution imaging reveals that AMPA receptors inside synapses are dynamically organized in nanodomains regulated by PSD95. J Neurosci 33 (32):13204–13224
31. Giannone G et al (2013) High-content superresolution imaging of live cell by uPAINT. Methods Mol Biol 950:95–110
32. Kechkar A et al (2013) Real-time analysis and visualization for single-molecule based superresolution microscopy. PLoS One 8(4):e62918
33. Tinevez JY et al (2017) TrackMate: an open and extensible platform for single-particle tracking. Methods 115:80–90
34. Kubala MH et al (2010) Structural and thermodynamic analysis of the GFP:GFP-nanobody complex. Protein Sci 19 (12):2389–2401
35. Durisic N et al (2014) Single-molecule evaluation of fluorescent protein photoactivation efficiency using an in vivo nanotemplate. Nat Methods 11(2):156–162
36. Craig AM, Banker G (1994) Neuronal polarity. Annu Rev Neurosci 17:267–310
37. Kaech S, Banker G (2006) Culturing hippocampal neurons. Nat Protoc 1(5):2406–2415
38. Chenouard N et al (2014) Objective comparison of particle tracking methods. Nat Methods 11(3):281–289
39. Izeddin I et al (2012) Wavelet analysis for single molecule localization microscopy. Opt Express 20(3):2081–2095

40. Racine V et al. (2006) Multiple-target tracking of 3D fluorescent objects based on simulated annealing. In: 2006 3rd IEEE international symposium on biomedical imaging: macro to nano, vol 1–3, pp 1020–1023
41. Kerr RA et al (2008) Fast Monte Carlo simulation methods for biological reaction-diffusion systems in solution and on surfaces. SIAM J Sci Comput 30(6):3126
42. Wilhelm BG et al (2014) Composition of isolated synaptic boutons reveals the amounts of vesicle trafficking proteins. Science 344 (6187):1023–1028
43. Mutch SA et al (2011) Protein quantification at the single vesicle level reveals that a subset of synaptic vesicle proteins are trafficked with high precision. J Neurosci 31(4):1461–1470
44. Takamori S et al (2006) Molecular anatomy of a trafficking organelle. Cell 127(4):831–846
45. Meunier FA et al (2010) Sustained synaptic-vesicle recycling by bulk endocytosis contributes to the maintenance of high-rate neurotransmitter release stimulated by glycerotoxin. J Cell Sci 123(Pt 7):1131–1140
46. Nwabuisi-Heath E, LaDu MJ, Yu C (2012) Simultaneous analysis of dendritic spine density, morphology and excitatory glutamate receptors during neuron maturation in vitro by quantitative immunocytochemistry. J Neurosci Methods 207(2):137–147
47. Grillo FW et al (2013) Increased axonal bouton dynamics in the aging mouse cortex. Proc Natl Acad Sci U S A 110(16):E1514–E1523
48. Truckenbrodt S, Rizzoli SO (2015) Synaptic vesicle pools: classical and emerging roles. In: Mochida S (ed) Presynaptic terminals. Springer, Tokyo
49. Iwabuchi S et al (2014) Examination of synaptic vesicle recycling using FM dyes during evoked, spontaneous, and miniature synaptic activities. J Vis Exp (85)
50. Raingo J et al (2012) VAMP4 directs synaptic vesicles to a pool that selectively maintains asynchronous neurotransmission. Nat Neurosci 15(5):738–745
51. Hua Z et al (2011) v-SNARE composition distinguishes synaptic vesicle pools. Neuron 71(3):474–487
52. Pan PY, Marrs J, Ryan TA (2015) Vesicular glutamate transporter 1 orchestrates recruitment of other synaptic vesicle cargo proteins during synaptic vesicle recycling. J Biol Chem 290(37):22593–22601
53. Kwon SE, Chapman ER (2011) Synaptophysin regulates the kinetics of synaptic vesicle endocytosis in central neurons. Neuron 70 (5):847–854
54. Granseth B et al (2006) Clathrin-mediated endocytosis is the dominant mechanism of vesicle retrieval at hippocampal synapses. Neuron 51(6):773–786
55. Voglmaier SM et al (2006) Distinct endocytic pathways control the rate and extent of synaptic vesicle protein recycling. Neuron 51(1):71–84
56. Ramirez DM et al (2012) Vti1a identifies a vesicle pool that preferentially recycles at rest and maintains spontaneous neurotransmission. Neuron 73(1):121–134
57. Harper CB et al (2011) Dynamin inhibition blocks botulinum neurotoxin type A endocytosis in neurons and delays botulism. J Biol Chem 286(41):35966–35976
58. Pelkmans L et al (2004) Caveolin-stabilized membrane domains as multifunctional transport and sorting devices in endocytic membrane traffic. Cell 118(6):767–780
59. Haas BL et al (2015) Single-molecule tracking in live Vibrio cholerae reveals that ToxR recruits the membrane-bound virulence regulator TcpP to the toxT promoter. Mol Microbiol 96(1):4–13
60. Jiang M, Chen G (2006) High Ca2+-phosphate transfection efficiency in low-density neuronal cultures. Nat Protoc 1 (2):695–700
61. Zeitelhofer M et al (2007) High-efficiency transfection of mammalian neurons via nucleofection. Nat Protoc 2(7):1692–1704
62. Belevich I et al (2016) Microscopy image browser: a platform for segmentation and analysis of multidimensional datasets. PLoS Biol 14 (1):e1002340
63. Sudhof TC, Rothman JE (2009) Membrane fusion: grappling with SNARE and SM proteins. Science 323(5913):474–477
64. Chanaday NL, Kavalali ET (2018) Presynaptic origins of distinct modes of neurotransmitter release. Curr Opin Neurobiol 51:119–126
65. Maritzen T, Haucke V (2018) Coupling of exocytosis and endocytosis at the presynaptic active zone. Neurosci Res 127:45–52
66. Heller JP, Rusakov DA (2017) The nanoworld of the tripartite synapse: insights from super-resolution microscopy. Front Cell Neurosci 11:374
67. Monnier N et al (2015) Inferring transient particle transport dynamics in live cells. Nat Methods 12(9):838–840
68. Persson F et al (2013) Extracting intracellular diffusive states and transition rates from single-molecule tracking data. Nat Methods 10 (3):265–269